M. Herceg[1], J. L. Jørgensen[1], J. M. G. Merayo[1], T. Denver[1], P. S. Jørgensen[1], M. Benn[1], S. Kotsiaros[1], and J. E. P. Connerney[2,3]

[1]Technical University of Denmark (DTU), Lyngby, Denmark.

[2]Space Research Corporation, Annapolis, MD, United States

[3]NASA Goddard Space Flight Center, Greenbelt, MD, United States

Corresponding author: Matija Herceg (mher@space.dtu.dk)

Key Points:

- The µASC observations confirms Ganymede's magnetic lensing and indicate its impact on the particle population and the wake region.
- Ganymede exhibits relative decrease (up to 52%) in high energy particle flux which is central and symmetrical to the Ganymede position.
- The magnetic shadow of Ganymede has a width of ~26,000 km, or ~10 Ganymede radii.

Abstract

The micro Advanced Stellar Compass (µASC), an attitude reference for the Juno Magnetic Field investigation, also continuously monitors high energy particle fluxes in Jupiter's magnetosphere. The µASC camera head unit (CHU) shielding is sufficient to stop electrons with energy <15MeV. By recording the number of particles that penetrate µASC CHU shielding and deposit energy in the CCD sensor, the µASC functions as an energetic particle sensor with a detection threshold well above that of the Juno Energetic Particle Detector Instrument (JEDI) flown for that purpose. Radiation data gathered by the µASC is used to monitor the radiation environment of Jupiter and mapping of the trapped high energy particles. Comparison of the particle population around Jupiter with individual perijove particle observations reveals disturbances when Juno is traversing Ganymede's M-shell. We present highly energetic electrons interaction with Ganymede's magnetic field, magnitude and extend of the particle depletion associated with the Ganymede interaction.

Plain Language Summary

The µASC camera onboard Juno, that serves primary as an attitude reference spacecraft, also continuously monitors high energy particle fluxes in Jupiter's magnetosphere. These observations, captured by the µASC, reveal particle flux disturbances caused by the Jupiter's moon Ganymede, their extent and magnitude.

1 Introduction

NASA's Juno spacecraft entered polar orbit about Jupiter on July 4th, 2016 (Bolton et al., 2017) and has now completed the 35 science orbits of its primary mission, systematically mapping the 3D magnetosphere of Jupiter (*Bagenal et al., 2017*). Located on the tip of the one of Juno's three solar arrays, the

Magnetic Field Experiment, MAG (*Connerney et al., 2017*) carries an attitude sensor; the fully autonomous micro Advanced Stellar Compass (µASC) designed and built at the Technical University of Denmark. In addition to its primary attitude determination function, the µASC is a star camera with a broad range of observational capabilities made possible by its versatile design. These include optical imaging of solar system bodies, autonomous detection and tracking of objects (*Benn et al., 2017; Jorgensen et al., 2020*) and detection of the high energy particles (e.g., *Connerney et al., 2020*). Electrons with energy >15MeV, protons with energy >80MeV and heavier elements with energy <~GeV penetrate the heavily shielded optical head of the Camera Head Unit (CHU) and are detected by analysis of the CCD imagery; individual pixel counts are recorded in every telemetry packet sent to the spacecraft Command and Data Handling (C&DH) subsystem for eventual transmission to Earth. This data provides a continuous record of the energetic particle environment traversed by Juno. The observed particle flux distribution provides an excellent in-situ measurement of the global energetic particle environment and its interaction with the moons of Jupiter.

Juno regularly traverses M-shells of Galilean moons during its orbital motion around Jupiter and often observes variations in the energetic particle population associated with interactions between Jupiter's magnetosphere and the moons. These particle signatures may take many forms, displaying different characteristics for different moons, and are often heavily influenced by the angular separation ("phase angle") between Juno and the moon during transit. The motion of these charged particles within the magnetic field of Jupiter is periodic and depends on particle energy, pitch angle ( ) and strength of the magnetic field (B). Trapped charged particles execute motion along the magnetic field in three superimposed motions: gyro, bounce, and drift motion, as illustrated in *Figure 1.* This illustration traces the motion of a 20, 60 and 100 MeV electron injected with a pitch angle of 10 degrees in a magnetic field described by the JRM09 internal magnetic field (*Connerney et al., 2018*) combined with that of the magnetodisc (Connerney et al., 2020). We simulate the motion of electrons with these energies to span the spectrum of energetic particles that the ASC instrument is sensitive to.

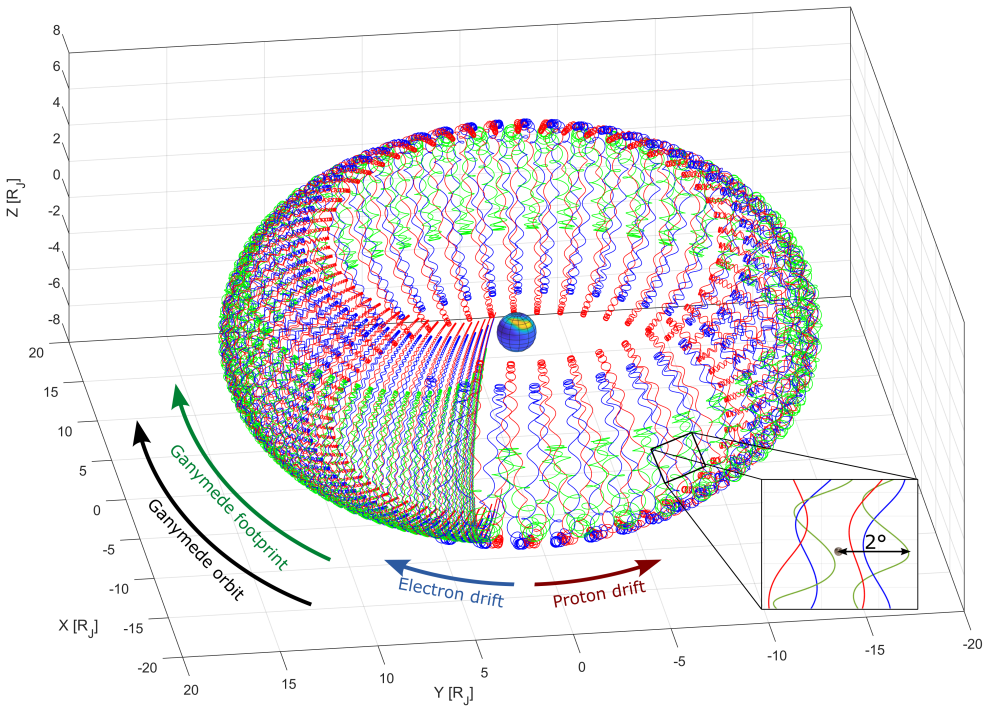

Figure 1: Motion of a 20 (green), 60 (blue) and 100 MeV (red) electron injected with an equatorial pitch angle of 10° at 15 R_J (Ganymede's orbital distance), bouncing between mirror points and slowly drifting westward around Jupiter with a drift period of 29, 87, and 144s respectively, and half bounce drift of ~2° along the magnetic equator.

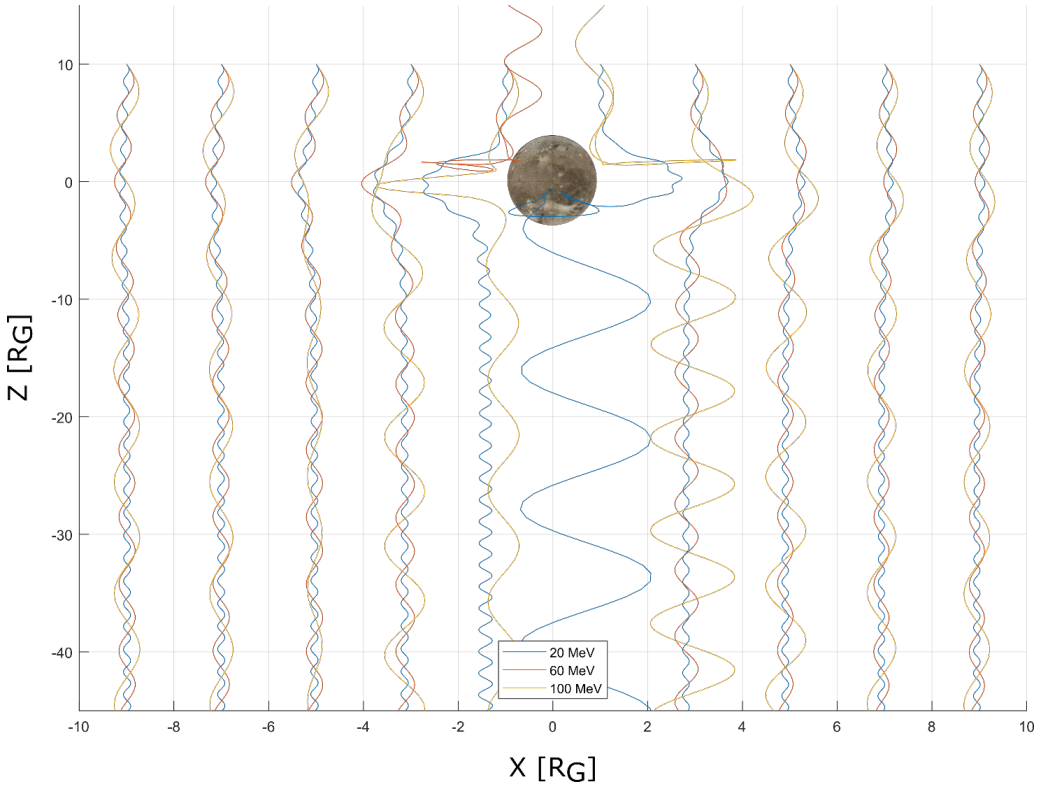

Figure 2: Computed energetic particle trajectories passing by Ganymede illustrating a particle shadow cast by the moon. Simulation uses electrons with energies of 20, 60 and 100MeV undergoing motion in a magnetic field computed using a Ganymede dipole and the Jovian magnetic field (JRM09 model).

In this paper, we focus on signatures observed by Juno's µASC when Juno is traversing Ganymede's M-shell, defined as the set of magnetic field lines that cross Jupiter's magnetic equator at Ganymede's radial distance from Jupiter. Similar to L-shell, calculated using the magnetic dipole (*Mcllwain, 1961*), an M-shell is computed using non-dipole fields.

To understand these signatures, we perform particle motion simulations for particles moving along field lines connecting the Juno spacecraft and Ganymede. Electron particle motion around Jupiter is governed by three adiabatic invariants, bouncing, gyration and westward drift motion (*Alfvén 1950, Northrop, 1966., Kruskal, 1958., Chew et. al, 1955*), as shown in *Figure 1.* North-south particle bouncing motion, also called the second adiabatic invariant, is expressed as the longitudinal integral between the two turning points for the particle trapped in a magnetic mirror. Particles with weaker energies have mirror points at lower latitudes and they drift faster (the third adiabatic invariant). If both the first and the second adiabatic invariants are conserved in the mag-

netic field, the particle will drift (the third adiabatic invariant) due to the radial gradient of the field ('gradient drift') and the curvature of the magnetic field lines ('curvature drift'). As the particle gyrates about the field, it will enter a weaker magnetic field when further from the planet causing it to drift east or west in longitude depending on the sign of its charge. Figure shows how the electron's equatorial pitch angle increases with eah bounce and the electron drifts more rapidly westward. A 60 MeV electron injected with 10° pitch angle at 15 R_J drifts around Jupiter in 87sec. Since each particle bounce between the mirror points increases the Larmor radius (gyration radius of circular motion), the drift rate increases also. This leads to the particle's loss of stability and it exits the drift shell after ~260 seconds. In the simulation, we do not account for the an energy loss mechanism such as synchrotron radiation and collisional loss.

A charged particle injected near Ganymede will be guided by the magnetic field of Jupiter (JRM09 model), the magnetodisc (*Connerney et al., 2020*) and the internal magnetic field of Ganymede (*Kivelson et al., 1997; Kivelson et al., 2002*). Particle motions were computed using the DTU particle simulation toolbox for the electrons with energies of 20, 60 and 100 MeV (*Figure2).* Verification of the DTU particle simulation toolbox was confirmed by comparison with previously published simulated particle trajectories (*Öztürk, 2012*). Nevertheless, uncertainties in particle trajectory calculations may be caused by accumulation of errors in numerical integration and the fidelity of the magnetic models used. Since particle motion is simulated 15R_J away from Jupiter, the magnetic model uncertainties are minimal but for variability of the magnetodisc. However, uncertainties in Ganymede's magnetic field (*Kivelson, 2002*) and those due to the interaction with Jupiter's field will directly impact simulated particle motions, and to a lesser extent, the total lensing effect.

Particle trajectory calculations were performed using JRM09 (*Connerney et al., 2018*) for Jupiter's field, augmented by a model magnetodisc (Connerney et al, 2020), and a Ganymede magnetic dipole model (*Kivelson, 2002*) with coefficients [g10, g11, h10] = [-728, 66, -11] nT. The field due to JRM09 and magnetodisc at Ganymede (~15 R_J)

is ~75nT, almost 10% of Ganymede's equatorial magnetic field; particle motion further away (>3 R_G) from Ganymede will be governed primarily by the magnetic field of Jupiter and the magnetodisc.

The simulation shows that electrons with energies of 20-100MeV passing within ~5 Ganymede radii (R_G) may be redirected up to ~4 R_G away from Ganymede, producing a particle "shadow" of up to ~8 $R_{G\ in}$ width. Juno has completed 35 orbits around Jupiter, having crossed Ganymede's M-shell more than 110 times. Even though the majority of these M-shell crossings occurred while Ganymede was well separated from Juno in longitude, a few crossings occurred with Juno and Ganymede in or near magnetic conjugacy. These few revealed a repeatable signature in the energetic particle population that illustrates the lensing effect that Ganymede's magnetic field has on particles of this energy.

2 Observations

The Juno spacecraft experiences multiple traversals of Ganymede's M-shell on approach to Jupiter, a consequence of its polar orbit and the ~10-hour rotation of Jupiter's magnetic field. These may occur at radial distances spanning Ganymede's orbital radius (14.96 RJ), their number and location largely determined by Juno's System III longitude on approach (Figure 3, right panel). When Juno crosses an M-shell corresponding to the orbit of one of Jupiter's moons, sensors on the spacecraft often detect variations in the charged particle environment (Sulaiman et al., 2020, Szalay et al., 2020, Paranicas et al., 2021), radio emissions (Louis et al., 2020), infrared observations (Mura et al., 2020), and magnetic field (Szalay et al., 2020) associated with the moon's interaction with the Jovian magnetosphere. The approach to Juno's 11th perijove presented a particularly auspicious opportunity to observe Ganymede's interaction with the magnetosphere, with numerous traversals of Ganymede's M-shell. Three of the traversals occurred while Juno and Ganymede were separated by a large radial distance (few to ~10 RJ) and within a few degrees of System III (1965) longitude. As shown in top left panel of figure 3, Juno's trajectory is illustrated with a black dashed line, and magnetic field lines that Juno crosses during the second Ganymede M-shell traversal are colored in red. The equatorial crossing point of the field line intersecting the spacecraft trajectory is marked with a blue line, while the equatorial crossing point of the field line passing through Ganymede's orbit is colored in red; both calculated using the JRM09 magnetic field model and the Connerney et al (2020) magnetodisc model. Where the two cross, Juno is traversing Ganymede's M-shell.

An overview of Juno's approach to perijove 11 appears in the top right panel of figure 3, a rendering in the magnetic dipole coordinate system. Juno traverses Ganymede's M-shell 5 times while inbound. Another way to illustrate M-shell traversals appears in the second row of figure 3, which shows the radial distance to the equatorial crossing point of the Juno spacecraft and the Galilean satellites as a function of time. Similarly, the third row shows the variation in time of the System III longitude of Juno and the major moons. Where Juno's and Ganymede's curves intersect in the second and third panel, Juno is traversing Ganymede's M-shell and on, or near, the same magnetic field line as Ganymede. This alignment is observed by μASC three times during perijove 11 (crossings 1, 2 and 3 on bottom of the figure 3).

Energetic particle flux observations (figure 3, bottom panel) show many features: a large, gradual increase in the particle population (between crossing 1 and 2) as Juno approaches the magnetic equator between the orbits of Ganymede and Europa; passage through the radiation belt "horn" right after crossing 3 at a distance of a few RJ; passage through perijove and again crossing of the radiation belt horn while outbound, this time much closer to Jupiter where the radiation is most intense. Apart from these large and expected radiation signatures, there a several small disturbances. Disturbances observed around perijove mapping to high magnetic latitudes are mostly associated with crossing of the

main aurora oval (Kotsiaros et al., 2019, Mauk et al., 2020) and episodic particle events mapping to very large radial distances (paper in preparation by DTU). The signatures we are concerned with here are those observed prior to perijove (marked 1, 2, 3) that correspond to the predicted traversal of Ganymede's M-shell depicted in the second and the third panels.

Juno traverses M-shells with different radial distances on approach to Jupiter. During perijove 11, at around 01:55 UTC and radial distance of 13 RJ, Juno's footprint meets the one of Ganymede (figure 3). Then, Juno and Ganymede have the same equatorial crossing distance (purple and blue line on the second row plot of figure 3). At nearly the same time a significant (~25%) decrease in energetic particle flux is observed by the μASC (bottom plot in figure 3). Similarly, at 06:47 UTC, Juno traverses Ganymede's M-shell even closer in phase (difference between the crossings S3 longitude) and observes a significant depletion (~50%) in particle flux. The third traversal occurs at 09:05 UTC, but by then the Juno and Ganymede field lines are separated by ~13 degrees S3 longitude resulting in a much weaker energetic particle depletion.

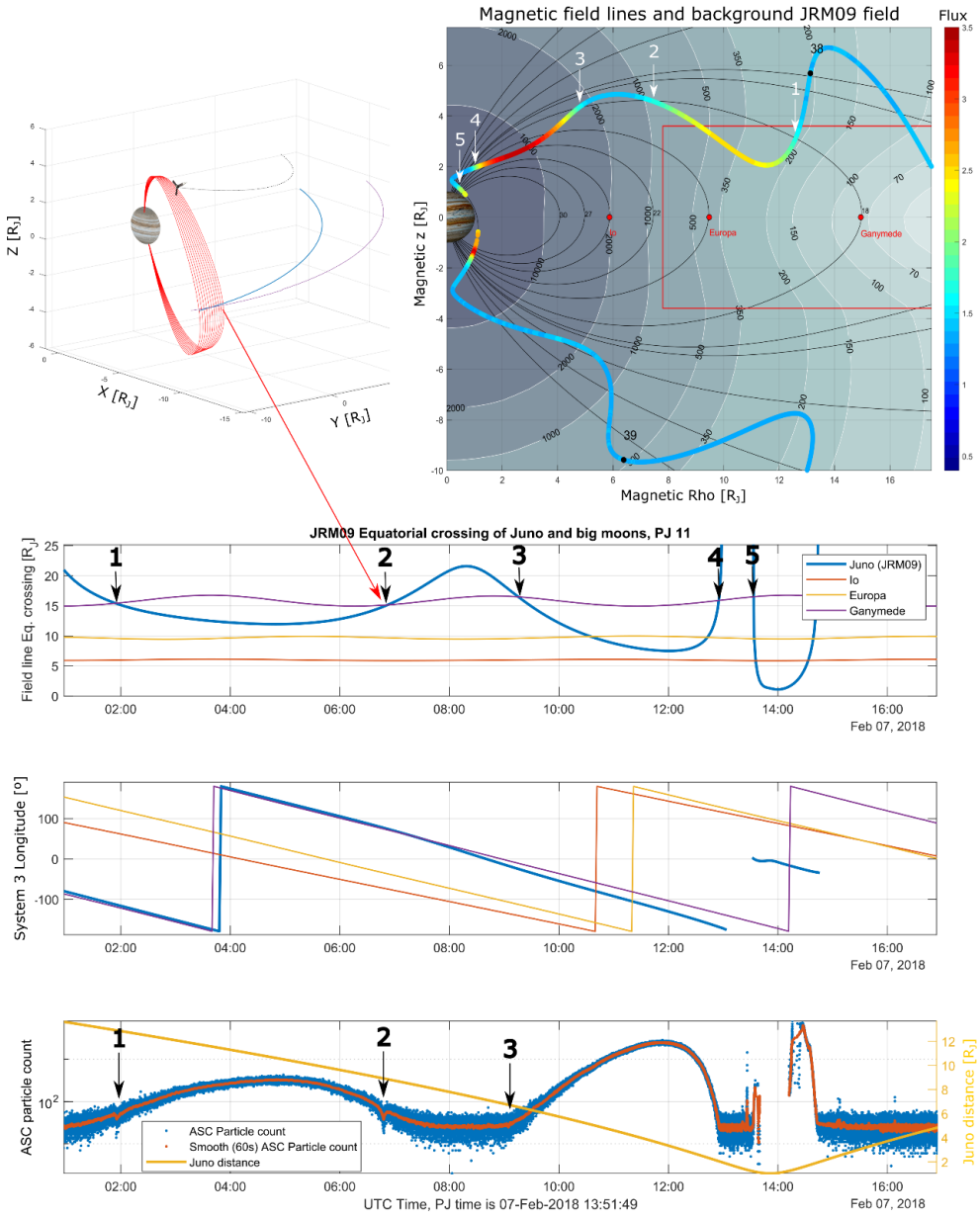

Figure 3: Observed particle flux disturbance due to Ganymede. Left top panel illustrates the geometry during event #2, during which Juno's equatorial crossing point crosses Ganymede's; magnetic field lines (red) intersecting the Juno trajectory (dashed black) and magnetic equator (blue). The top right panel shows Juno's trajectory in magnetic equatorial coordinates color coded with the intensity of radiation observed by the μASC. Bottom 3 panels show satellite and

spacecraft equatorial crossing distance, S3 longitude, and µASC observations as a function of time (blue and red, averaged). Ganymede interaction events 1, 2, and 3 indicated.

µASC observations displayed in the bottom plot of figure 3 show clear signatures of Ganymede's interaction with the charged particle environment. However, the signatures of the highly energetic particles that µASC is sensitive to (>20 MeV) are only observed when Ganymede and Juno have small phase separation.

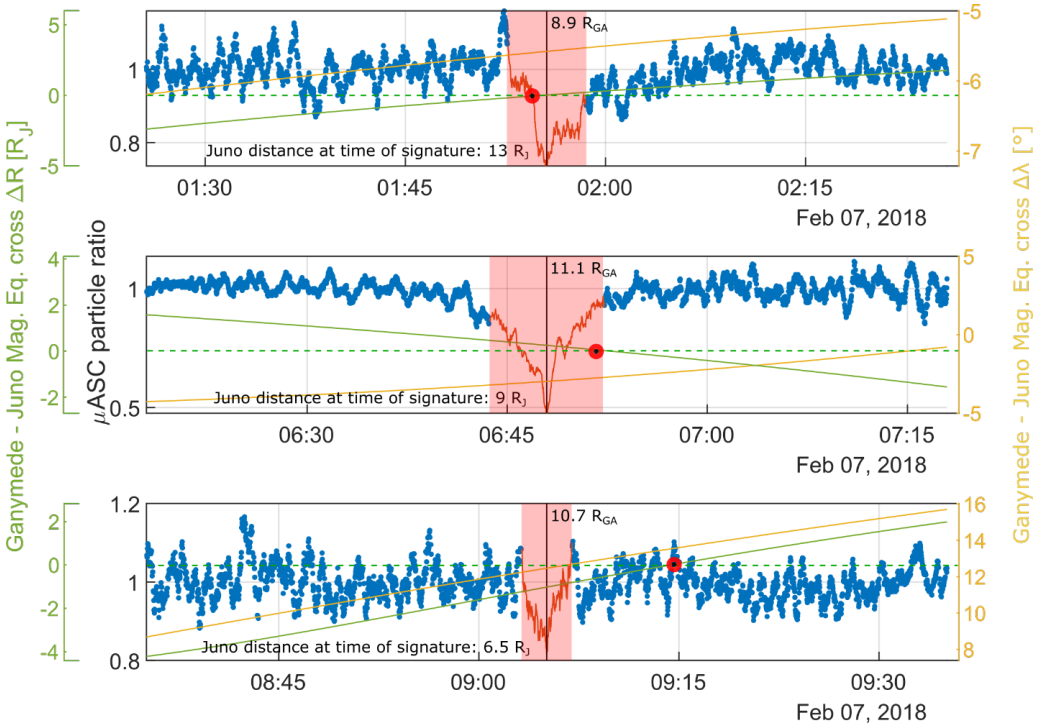

Figure 4: Three panels show µASC observations as a function of time (1, 2, 3, from top to bottom). The green line shows the difference in the radial direction (Rj) between the equatorial crossing point of field lines through Ganymede and Juno, and the yellow line shows angular difference. Red shaded area spans the Ganymede signature and the red filled circle indicates where the model predicts the crossing of Juno and Ganymede M-shells.

4 Results

Juno observes a depletion of energetic particles, presumably electrons, when it traverses magnetic field line that connected (or close) to Ganymede. A depletion of ~15-50% in particle count is observed and the magnitude of the depletion depends on the phase angle, with a reduction of 50% experienced at small (-2.5 deg) phase angle, and 15% at larger (-13 deg) phase angle. Traversals of Ganymede's M-shell that occur with greater phase separation (>~10^o SIII

longitude) evidence no particle depletion. These signatures could alternatively be explained by the presence of a cloud of neutrals around Ganymede, closely confined to Ganymede's position, depleting the energetic electrons within the μASC sensitivity band (15-80MeV).

The particle depletion is similar in spatial scale for all 3 events, varying between 8.9 and 11.1 Ganymede radii (R_{GA}). The time spent in the particle depletion region is dictated by the angle between Juno's and Ganymede's magnetic equator crossing footprints; if small the depletion persists longer.

The width of the depletion region can be compared to the simulations to illustrate the Ganymede lensing effect (figure 2). The simulation shows a Ganymede magnetic "shadow" of ~8 R_{GA}, compared to the average observed width of ~10 R_{GA}. The small difference between model and observation could be due to other contributors to the measured particle flux, or temporal variation in the magnetic field, not captured by the models.

Juno's μASC observations of Ganymede particle depletion show that magnetic shadowing effect is present up to ~13^{o} separation in phase. However, at this distance the signature is very weak and at the edge of μASC detection sensitivity, as in the plot for perijove 1 (figure 5). The stronger particle depletion observed when Juno is trailing Ganymede can be explained by the wake flow and magnetospheric plasma not filling the Ganymede particle trail, compared to the plasma density in Ganymede's ram direction. Signatures might also originate from the wake region, if accounting for the bend back of the field due to radial currents and half bounce drift (as shown on figure 1).

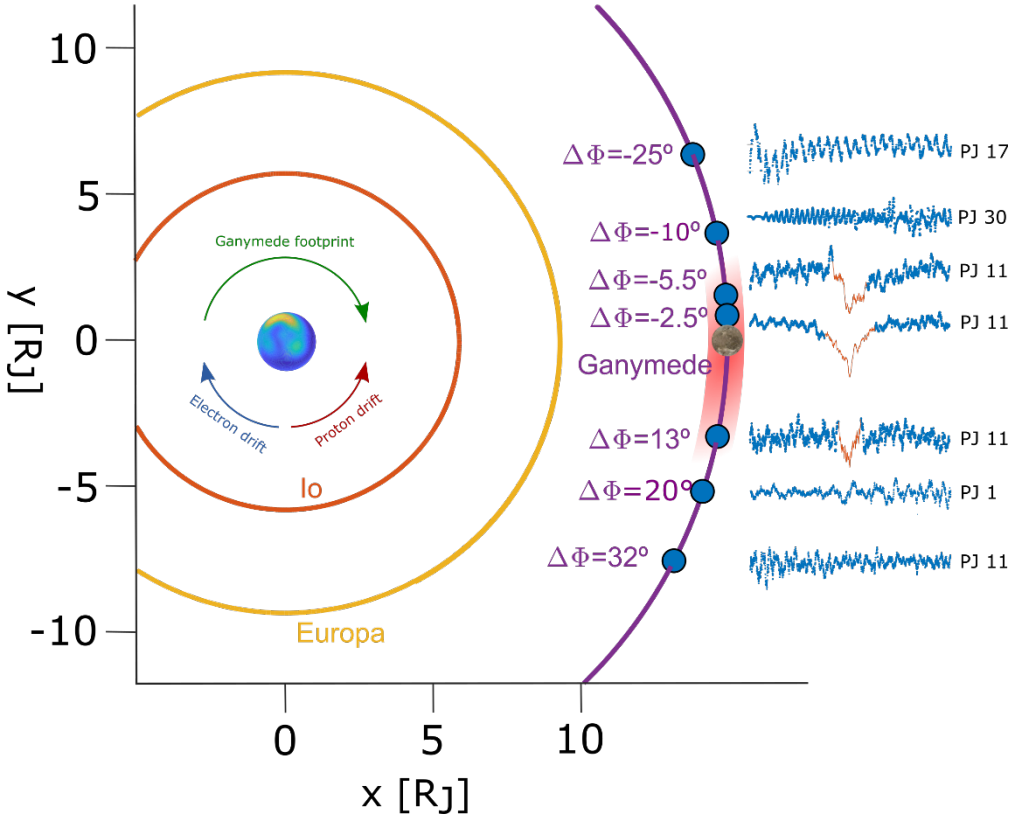

Figure 5: Footprint of the Galilean moons in the magnetic equator and the associated depletion of the high energy particle population. Dots (blue filled circles) mark the S3 longitude of the equatorial crossing point of the field line through Juno as Juno transverses the Ganymede M-shell. Shaded area shows how far away in S3 longitude the particle shadow is observed in the radiation data, illustrated (blue) to the right. Negative indicates when Juno footprint is trailing Ganymede.

Thus far during Juno's prime mission, there have been more than 120 traversals of Ganymede's M-shell. Of these only a handful with small phase separation show clear signatures (figure 5). Our analysis, supported by the simulations of energetic electron motion in the environment of Ganymede, shows that the magnetic shadow of Ganymede has a width of ~26,000 km, or ~10 Ganymede radii. This novel use of the µASC star tracker as an energetic particle detector, and observations obtained in the Ganymede environment, allows us to constrain the energy of the population penetrating the µASC. The particle trajectory calculations suggest that the µASC mainly observes ~80 MeV electrons at the Ganymede M-shell distances.

5 Conclusions

During 35 successful science orbits of its primary mission, Juno's Advanced Stellar Compass (μASC) continuously monitored the population of high energy particles (>15MeV electron and <80MeV protons) in Jupiter's magnetosphere. Comparison of the particle population model around Jupiter with individual perijove particle observations reveals disturbances observed when Juno is traversing M-shell of Ganymede. Particle fluxes observed while traversing Ganymede M-shell are heavily influenced by the phase angle between Juno and Ganymede.

The μASC observations confirm the presence of the Ganymede magnetic lensing and its extent along the wake region. Ganymede causes a relative decrease (up to 52%) in high energy particle flux which is central and symmetrical to Ganymede's position, supported by simulations of energetic electron motion in Ganymede's environment. These simulations show that the magnetic shadow of Ganymede has a width of ~26,000 km, or ~10 Ganymede radii. Close agreement between Ganymede magnetic lensing simulation and μASC observations confirms that the JRM09 and current sheet model fits very well with observations and can be reliably used for magnetic field tracing and M-shell definition within the inner (<30 R_J) inner magnetosphere. The μASC observations are a useful complement to Juno's dedicated radiation monitoring instruments, extending detection capability to particle energies > 20 MeV.

Acknowledgments

All authors acknowledge support from the Juno project. Data supporting the conclusions are available in the permanent archival data repository, Zenodo (Herceg et al, 2021), and will soon be archived in the NASA Planetary Data System at https://pds.nasa.gov,

References

Alfvén, It., Cosmical Electrodynamics, Clarendon Press, Oxford, (1950).

Bagenal, F., Adriani, A., Allegrini, F., Bolton, S.J., Bonfond, B., Bunce, E.J., et al. (2017). Magnetospheric science objectives of the Juno mission. *Space Science Reviews*. doi:10.1007/s11214-014-0036-8.

Benn, M., Jorgensen, J.L., Denver, T., Brauer, P., Jorgensen, P.S., Andersen, A.C., et al. (2017), Observations of interplanetary dust by the Juno magnetometer investigation*, Geophys. Res. Lett., 44,* doi:10.1002/2017GL073186.

Bolton, S.J., Lunine, J., Stevenson, D. *et al.* The Juno Mission. *Space Sci Rev* **213,** 5–37 (2017). https://doi.org/10.1007/s11214-017-0429-6

Bonfond, B., Hess, S., Bagenal, F., Gérard, J. C., Grodent, D., Radioti, A., Gustin, J., & Clarke, J. T. (2013). The multiple spots of the Ganymede auroral footprint. *Geophysical Research Letters*, 40, 4977– 4981. http://doi.org/10.1002/grl.50989

Bonfond, B., Saur, J., Grodent, D., Badman, S. V., Bisikalo, D., Shematovich, V., Gérard, J. C., & Radioti, A. (2017). The tails of the satellite auroral foot-

prints at Jupiter. *Journal of Geophysical Research: Space Physics*, 122, 7985–7996. http://doi.org/10.1002/2017JA024370

Chew, G. F., M. Goldberger, F. Low (1955) The individual particle equations of motion in the adiabatic approximation. *Los Alamos Sci. Lab. Rept. LA-2055*, chapter T-759,

Connerney, J.E.P., Benn, M., Bjarno, J.B. *et al.* The Juno Magnetic Field Investigation. *Space Sci Rev* **213,** 39–138 (2017). https://doi.org/10.1007/s11214-017-0334-z

Connerney, J. E. P., Kotsiaros, S., Oliversen, R. J., Espley, J. R., Joergensen, J. L., Joergensen, P. S., Merayo, J. M. G., Herceg, M., Bloxham, J., Moore, K. M., Bolton, S. J., & Levin, S. M. (2018). A new model of Jupiter's magnetic field from Juno's first nine orbits. *Geophysical Research Letters*, 45, 2590– 2596. https://doi.org/10.1002/2018GL077312

Connerney, J. E. P., Timmins, S., Herceg, M. & Jørgensen, J. L. (2020) A Jovian Magnetodisc Model for the Juno Era. In: *Journal of Geophysical Research: Space Physics*. 125, 10, 11 p., e2020JA028138.

M. Herceg, J. L. Jørgensen, J. M. G. Merayo, T. Denver, P. S. Jørgensen, M. Benn, S. Kotsiaros, & J. E. P. Connerney (2021) Supplementary material for *Energetic Electron Imaging of Ganymede's Magnetic Field by the Juno Spacecraft's Advanced Stellar Compass*, Zenodo DOI: https://doi.org/10.5281/zenodo.5503852

Jorgensen, J. L., Benn, M., Connerney, J. E. P., Denver, T., Jorgensen, P. S., Andersen, A. C., & Bolton, S. J. (2020). Distribution of interplanetary dust detected by the Juno spacecraft and its contribution to the Zodiacal Light. *Journal of Geophysical Research: Planets*, *125*, e2020JE006509. https://doi.org/10.1029/2020JE006509

Kivelson, M. G., Khurana, K. K., Coroniti, F. V., et al. (1997). The magnetic field and magnetosphere of Ganymede. *Geophysical Research Letters* **24**: 2155-2158.

Kivelson, M. G., Khurana, K., and Volwerk, M. (2002). The permanent and inductive magnetic moments of Ganymede. *Icarus* **157:** 507-522.

Kotsiaros, S., Connerney, J. E. P., and Martos, Y. (2020). Analysis of Eddy current generation on the Juno spacecraft in Jupiter's magnetosphere, *Earth and Space Science*, doi:10.1029/2019EA001061

Kotsiaros, S., Connerney, J.E.P., Clark, G. et al. Birkeland currents in Jupiter's magnetosphere observed by the polar-orbiting Juno spacecraft. *Nat Astron 3*, 904–909 (2019). https://doi.org/10.1038/s41550-019-0819-7

Kruskal, M. (1958) The gyration of a charged particle. *Project Matterhorn Rept.* PM-S-33 (NYO7903), Princeton University. March.

Louis, C.K., Louarn, P., Allegrini, F., Kurth, W.S. and Szalay, J.R., 2020. Ganymede-Induced Decametric Radio Emission: In Situ Observations and Measurements by Juno. *Geophysical Research Letters*, 47(20), p.e2020GL090021

Mauk, B. H., Clark, G., Gladstone, G. R., Kotsiaros, S., Adriani, A., Allegrini, F., et al. (2020). Energetic particles and acceleration regions over Jupiter's polar cap and main aurora; a broad overview. *Journal of Geophysical Research: Space Physics*, 125. https://doi.org/10.1029/2019JA027699

McIlwain, Carl E. (1961) Coordinates for Mapping the Distribution of Magnetically Trapped Particles, *Journal of Geophysical Research*, 66 (11): 3681–3691, Bibcode:1961JGR....66.3681M, doi:10.1029/JZ066i011p03681, hdl:2060/20150019302

Mura, A., et al. (2020), Infrared Observations of Ganymede From the Jovian InfraRed Auroral Mapper on Juno, *Journal of Geophysical Research (Planets)*, **125**, e06508, doi:10.1029/2020JE006508

Northrop T.G. (1966) Adiabatic Theory of Charged Particle Motion. In: McCormac B.M. (eds) Radiation Trapped in the Earth's Magnetic Field. Astrophysics and Space Science Library (A Series of Books on the Developments of Space Science and of General Geophysics and Astrophysics Published in Connection with the *Journal Space Science Reviews*), vol 5. Springer, Dordrecht. https://doi.org/10.1007/978-94-010-3553-8_3

Öztürk, M. K., (2012). Trajectories of charged particles trapped in Earth's magnetic field, *American Journal of Physics* 80, 420; https://doi.org/10.1119/1.3684537

Paranicas, C., et al. (2021), Energy Spectra Near Ganymede From Juno Data, *Geophysics Research Letters*, **48**, e93021, doi:10.1029/2021GL093021.

Sulaiman, A.H., Hospodarsky, G.B., Elliott, S.S., Kurth, W.S., Gurnett, D.A., Imai, M., Allegrini, F., Bonfond, B., Clark, G., Connerney, J.E.P. and Ebert, R.W., 2020. Wave-particle interactions associated with Io's auroral footprint: Evidence of Alfvén, ion cyclotron, and whistler modes. *Geophysical Research Letters,* 47(22), p.e2020GL088432

Szalay, J.R., et al. (2020), Alfvénic Acceleration Sustains Ganymede's Footprint Tail Aurora, *Geophysics Research Letters*, **47**, e86527, doi:10.1029/2019GL086527